

which implies

$$\cos\omega = k(1+b^2)^{-\frac{1}{2}} \sin u, \quad \sin\Omega = bk(b^2 + \operatorname{dn}^2 u)^{-\frac{1}{2}} \sin u, \quad (36)$$

$$d\omega/dx = -k(-g)^{\frac{1}{2}}(b^2 + \operatorname{dn}^2 u)^{-\frac{1}{2}} \operatorname{cn} u \operatorname{dn} u, \quad (37)$$

$$\sin\omega(d\Omega/dx) = bk(-g)^{\frac{1}{2}}(b^2 + \operatorname{dn}^2 u)^{-\frac{1}{2}} \operatorname{cn} u, \quad (38)$$

$$V = 4\pi J_s(-g)^{-\frac{1}{2}}(\operatorname{am} u + C), \quad (39)$$

where  $C$  is a constant.

Using (37) and (38) in (9), one obtains that either  $bk=0$ , or  $\operatorname{cn} u=0$ , for  $x=\pm a$ . Suppose the latter is possible; then

$$u(a) = (2n+1)K(k), \quad u(-a) = (2m+1)K(k), \quad (40)$$

where  $m$  and  $n$  are integers. In this case

$$\operatorname{am} u(a) = (n + \frac{1}{2})\pi, \quad \operatorname{am} u(-a) = (m + \frac{1}{2})\pi.$$

Substituting in (39),  $V$  cannot fulfill (32a) unless  $m=n$  and according to (40) and (35) this is impossible. It follows that the only possibility is  $bk=0$ . Now if  $k=0$ , one obtains from (36) that  $\sin\Omega=0$  and according to (14)

$$b=0. \quad (41)$$

It can now be shown that the only solution of (7) which fulfills the boundary conditions is  $\sin 2\omega=0$ .

## Recovery of Electron Radiation Damage in $n$ -Type InSb\*

F. H. EISEN

*Atomics International, Division of North American Aviation, Inc., Canoga Park, California*

(Received March 22, 1961)

The production and recovery of electron radiation damage in  $n$ -type InSb has been studied by means of Hall-coefficient and electrical-conductivity measurements. Irradiations were performed mainly at 80°K, since no recovery was observed between 4° and 80°K. The damage recovered in five well-defined stages with the recovery nearly complete at 320°K. Isochronal and isothermal recovery was monitored in each of the stages, allowing a determination of the activation energies for recovery and a study of the recovery kinetics. None of the recovery kinetics fit any simple models. There is evidence that the two lowest-temperature recovery stages involve the annihilation of close interstitial-vacancy pairs and that interactions of primary defects with impurities do not occur. However, the first-order kinetics expected for close-pair recovery is not explicitly observed. A possible explanation for the observed kinetics, involving the independent annihilation of two types of close-pair configurations in the same stage with an electrostatic interaction between the interstitial and vacancy, is proposed.

### I. INTRODUCTION

THE recovery of electron radiation damage has been studied in some detail in germanium<sup>1,2</sup> and to a lesser extent in silicon.<sup>1,3</sup> Aukerman<sup>4</sup> has published some results on damage recovery in InSb; however, the present work probably represents the first extensive study of damage recovery in a compound semiconductor.

The production of damage in  $n$ -type InSb by electrons with energies as low as 0.24 Mev (corresponding to a maximum energy transfer to an indium atom of 5.7 ev) has been reported earlier.<sup>5</sup> The present paper reports a detailed study of recovery of electron radiation damage produced principally at 0.4, 0.7, and 1.0 Mev. The results are mainly concerned with recovery in samples with initial electron concentrations of about  $1.5 \times 10^{16}$

cm<sup>-3</sup>, and, unless specified otherwise, the results quoted are for such samples. Some differences which occur when purer samples are used are also mentioned, and these effects are the subject of further investigations.

InSb crystallizes in the zincblende structure. In this structure, each indium atom is tetrahedrally surrounded by four antimony atoms, and each antimony is similarly surrounded by four indium atoms. The indium atoms and antimony atoms each lie on a fcc sublattice, and there are two more sublattices of vacant sites. One of these has tetrahedrally arranged indium atoms for nearest neighbors, and the other has nearest neighbor antimony atoms in the same arrangement. This leads to four possible interstitial configurations, i.e., an indium interstitial with either indium or antimony nearest neighbors and similar configurations for an antimony interstitial. There are also two possible kinds of vacancies and two kinds of replacements in which the originally displaced atom strikes an atom of the other type displacing it and remaining in its lattice position.

One might think that this multiplicity of possible point defects would lead to complications in the radiation damage studies in InSb in comparison to elemental

\* Supported by the U. S. Atomic Energy Commission.

<sup>1</sup> W. L. Brown, W. M. Augustyniak, and T. R. Waite, *J. Appl. Phys.* **30**, 1258 (1959).

<sup>2</sup> J. W. MacKay and E. E. Klontz, *J. Appl. Phys.* **30**, 1269 (1959).

<sup>3</sup> G. Bemski and W. M. Augustyniak, *Phys. Rev.* **108**, 645 (1957).

<sup>4</sup> L. W. Aukerman, *Phys. Rev.* **115**, 1125 (1959).

<sup>5</sup> F. H. Eisen and P. W. Bickel, *Phys. Rev.* **115**, 345 (1959).

semiconductors. In fact, the behavior seems in some ways simpler. For instance, there are good indications that reactions with impurities do not play the important role they do in germanium<sup>1</sup> and silicon,<sup>6</sup> and the effects of irradiation temperature on damage rate are much simpler in InSb than in germanium.<sup>1</sup> Five recovery stages have been observed with nearly complete recovery occurring when temperatures of 320°K are reached. Above this temperature, there remains a small change in resistivity. Although the results are not completely interpretable at present, there are indications that the recovery stages are independent of each other and do not involve interactions of radiation-induced defects with impurities and that at least two of the stages are due to the recovery of close interstitial-vacancy pairs.

## II. EXPERIMENTAL TECHNIQUES

The experiments were carried out by irradiating thin samples of InSb mounted in a target box attached to the Van de Graaff accelerator. Irradiations and electrical measurements were usually performed at liquid-nitrogen temperature. In cases where recovery close to liquid-nitrogen temperature was to be observed, the temperature rise of the sample during irradiation was limited to about 2°K. If only higher temperature recovery was to be measured, a greater temperature rise was allowed. Isothermal and isochronal recovery data were obtained by heating the sample to the annealing temperature, holding it there for the desired time, and returning it to liquid-nitrogen temperature for measurement of Hall coefficient and electrical resistivity. This cycle was repeated for each point on the recovery curve. Isochronal annealing pulses were of 5-min duration; the temperature increase between successive pulses was constant in a given recovery stage and was usually 5°K.

The samples were fabricated with arms for attaching Hall-coefficient and resistivity leads. They were 1 to 2 mm wide (exclusive of the contact arms), 8 to 12 mm long, and 90 to 200  $\mu$  thick. The desired shape was obtained by masking the sample area and removing the surrounding material using an S. S. White airbrasive unit. They were then polished to the required thickness, and, in some cases, the surface layers were removed by etching in dilute CP-4. No difference in recovery between etched and unetched samples was observed. Leads were attached by soldering, using ordinary soft solder and a zinc chloride flux. The almost complete recovery of damage after annealing made possible the use of one sample for several damage recovery experiments.

The target box, shown in Fig. 1, was used to maintain the sample in the vacuum of the vertically mounted Van de Graaff accelerator (about  $2 \times 10^{-6}$  mm Hg) and was provided with means of cooling the sample during irradiation and of heating for annealing. A solenoid *L* wound on the outside of the nonmagnetic stainless-steel

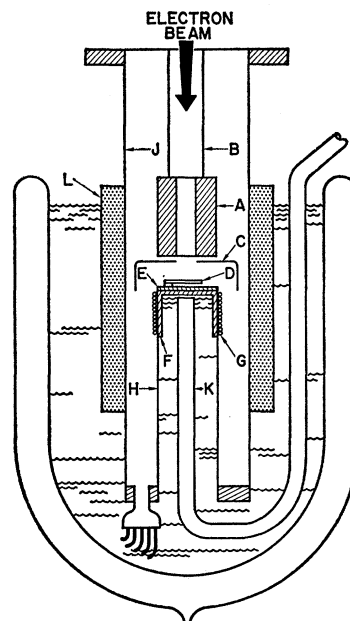


Fig. 1. Target box used in irradiating and annealing semiconductor samples. See text for explanation of symbols.

tube *J* provided the magnetic field for Hall-coefficient measurements. Irradiations at energies of 0.7 Mev or higher were performed through a 0.5-mil aluminum scatterer located 50 cm above the sample in order to achieve a uniform beam over the area of the sample. The slit *A* and tube *B* served to collimate the beam and prevent electrons from hitting the tube *J*. This was necessary in order to be able to collect and measure current passing through the slits since plate *E*, to which the sample *D* was soldered, was in direct contact with the copper piece *F* to obtain good thermal contact, and therefore, the sample and plate *E* were electrically connected to the tube *J*.

The target box was partially immersed in the coolant, and cooling was accomplished by venting the closed tube formed by *H* and *F* through the vent tube *K* so that the coolant could rise and make contact with *F*. To heat the sample, the vent tube was closed and the heater *G* turned on. This caused a gas bubble to form in the stainless-steel tube *H* so that there was no longer a good thermal path to the coolant from the sample. The heater *G* was wound on *F* and consists of about 50 turns of 3-mil manganin wire. With this heater and heat switch system, it was possible to achieve rapid enough heating and cooling of the sample so that little or no time correction to the annealing results is necessary. Temperature control was accomplished by applying the amplified difference between the control thermocouple voltage and an appropriately set opposing potentiometric voltage to a controller. Temperature control to about  $\pm 0.03$  degree could be maintained. *C* was thermally connected to *E* and served as a radiation

<sup>6</sup> G. D. Watkins and J. W. Corbett, Phys. Rev. **121**, 1001 (1961).

shield as well as forming part of the Faraday cage for beam collection and integration.

The Van de Graaff accelerator can be operated in the energy range from 0.2 to 2.0 Mev. The generating voltmeter of the accelerator was calibrated at 1.66 Mev against the threshold for photoproduction of neutrons in beryllium.<sup>7</sup>

The measurements of Hall coefficient and electrical resistivity were carried out by standard potentiometric methods. The current supply for the Hall-field solenoid was regulated using a circuit due to Garwin.<sup>8</sup> Temperature measurements were made by means of copper-constantan thermocouples attached to two of the sample arms. The thermocouples were calibrated against a platinum resistance thermometer.

### III. ACTIVATION ENERGY ANALYSIS

A value for the activation energy for damage recovery may be deduced from the combination of isochronal and isothermal recovery data for identical samples.<sup>9</sup> If  $p$  is that part of the measured property associated with the annihilating defects, one can determine the time  $\tau_i$  at which a value in the isothermal curve is reached equal to the value of  $p_i$  measured at the end of the  $i$ th pulse on the isochronal curve for an identical sample carried out at temperature  $T_i$ . According to this procedure, the important quantity to consider is not  $\tau_i$  but  $\Delta\tau_i = \tau_i - \tau_{i-1}$ . Any straight-line section obtained on a plot of  $\ln\Delta\tau_i$  vs  $1/T_i$  is characterized by a unique activation energy  $E$ , given by the expression

$$\ln\Delta\tau_i = C' - E/kT_i, \quad (1)$$

where  $C'$  is a constant and  $k$  is Boltzmann's constant. A sufficient condition for the validity of this analysis is that  $p$  be a monotonically increasing or decreasing function of the defect concentration. If the recovery obeys the chemical rate equation,

$$dp/dt = -\nu p^\gamma e^{-E/kT}, \quad (2)$$

it is not necessary that the two samples be identical for Eq. (1) to be valid. In Eq. (2),  $\nu$  is the frequency factor and  $\gamma$  the order of the reaction.

### IV. RESULTS AND DISCUSSION

#### A. General Features of Damage Recovery

Damage produced by irradiation with 1-Mev electrons is expected to consist mainly of randomly located interstitial-vacancy pairs with a distribution of interstitial-vacancy spacings which depends on the energy of irradiation.<sup>10</sup> Recovery of the damage will depend on

this interstitial-vacancy spacing, and one would expect to obtain information relative to it from observation of the kinetics of damage recovery. Discussion of this recovery will be facilitated by the introduction of the concept of the capture radius defined as the maximum separation of the interstitial and vacancy at which annihilation must occur if one of the defects is mobile. If the separation of the interstitial and vacancy is less than a capture radius, the pair may not be stable at any temperature. If it is stable at the temperature of irradiation, the interstitial and vacancy will annihilate when the sample is annealed to a temperature at which one of the defects becomes mobile. If the separation is greater than the capture radius, the motion of the interstitial (considering it as the mobile defect) will be described by a random walk process, and it may recombine with the vacancy from which it was dislodged or wander through the lattice to recombine with another vacancy. The magnitude of the capture radius will depend on the lattice distortion in the neighborhood of the defects and on possible electrostatic interactions between the interstitial and vacancy.

Interstitials within a capture radius of a vacancy are expected to become mobile at lower temperatures than those outside the capture radius since the potential-energy barrier for migration is expected to be lower due to the proximity of a vacancy. The decay of these close pairs is generally expected to obey first-order kinetics. This should be strictly so only if the interstitial has to make a single jump to recombine with its vacancy. If two or more jumps are required for annihilation and the jump frequency for the first jump is considerably lower than for succeeding jumps, the kinetics will remain first-order within the precision of measurement. This may be expected to hold in the case where the potential-energy barriers for interstitial migration decrease markedly on approach to the vacant lattice site. However, if two or more rate determining jumps with about the same jump frequency are required, the kinetics will deviate considerably from first order.

The recovery kinetics for pairs separated by distances greater than a capture radius has been treated by Fletcher and Brown<sup>11</sup> and by Waite.<sup>12</sup> In general, there are two stages in this recovery. During the first, there is still a correlation between the interstitials and vacancies from which they were dislodged, and the fraction of interstitial-vacancy pairs which have annihilated is initially proportional to the square root of time of anneal. After the correlated recovery has occurred, the remaining vacancies and interstitials recombine at random, leading to a second-order process. Both of these stages have been observed following low-temperature irradiation of copper.<sup>13</sup> In addition to the recombination of interstitials and vacancies, it is possible that the

<sup>7</sup> R. C. Mobley and R. A. Laubenstein, Phys. Rev. **80**, 309 (1950).

<sup>8</sup> R. L. Garwin, Rev. Sci. Instr. **29**, 223 (1958).

<sup>9</sup> C. J. Meehan and J. A. Brinkman, Phys. Rev. **103**, 1193 (1956).

<sup>10</sup> For a discussion of damage production and recovery see G. J. Dienes and G. H. Vineyard, *Radiation Effects in Solids* (Interscience Publishers, Inc., New York, 1957).

<sup>11</sup> R. C. Fletcher and W. L. Brown, Phys. Rev. **92**, 585 (1953).

<sup>12</sup> T. R. Waite, Phys. Rev. **107**, 471 (1957).

<sup>13</sup> J. W. Corbett, R. B. Smith, and R. M. Walker, Phys. Rev. **114**, 1452 (1959).

recovery may be complicated by the formation of defect-impurity complexes and multiple defects such as divacancies or di-interstitials. Defect-impurity complexes seem to be formed during recovery in germanium<sup>1</sup> and are a product of room-temperature irradiation of silicon.<sup>6</sup>

### B. General Features of the Data

The carrier concentration in the InSb samples was determined from the relation  $n=1/Re$ , where  $n$  is the carrier concentration,  $R$  the Hall coefficient, and  $e$  the electron charge. The defects introduced by electron irradiation of  $n$ -type InSb act as net acceptors since the carrier concentration is decreased as a result of the irradiation. The carrier concentration removed  $\Delta n$  depends linearly on the integrated beam current at 1 Mev with a carrier removal rate of  $8.6 \text{ cm}^{-1}$  (electrons  $\text{cm}^{-3}/\text{bombarding electron cm}^{-2}$ ). This linear dependence holds at least to  $\Delta n/n_0=0.5$ , the largest value used in this work, and indicates that  $\Delta n$  is proportional to the number of defects introduced by the irradiation;  $\Delta n$  is used as the measure of damage in this paper. The frac-

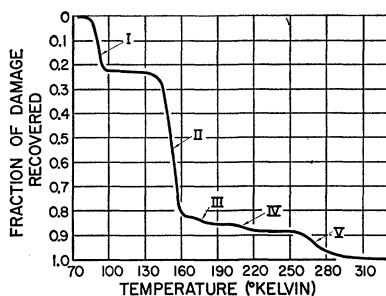


FIG. 2. Isochronal recovery curve showing stages I to V as labeled. The heating rate was  $\frac{1}{2}^\circ\text{K}/\text{min}$  in stage I and  $1^\circ\text{K}/\text{min}$  in stages II to V.

tion of damage not recovered is then given by the ratio of  $\Delta n$  remaining after a given annealing treatment to the total  $\Delta n$  for the irradiation.

The isochronal recovery curve for a sample irradiated at liquid-nitrogen temperature with 1-Mev electrons is presented in Fig. 2, which shows five well-separated recovery stages. These will be referred to as stages I through V, as shown. Irradiation of the same sample at liquid-helium temperature with 0.7-Mev electrons resulted in the same carrier removal rate as for liquid-nitrogen temperature irradiations with 0.7-Mev electrons. Isochronal annealing revealed no recovery until the temperature region of stage I was reached. Irradiation at  $165^\circ\text{K}$  results in the same total carrier removal as if the sample were irradiated at liquid-nitrogen temperature and annealed to  $165^\circ\text{K}$  leaving only stages III-V. A similar result has been reported by Aukerman<sup>4</sup> for irradiation at  $200^\circ\text{K}$  where stages IV and V are stable.

The isothermal recovery data are shown in Fig. 3.

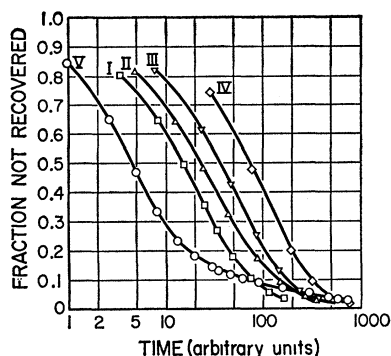


FIG. 3. Isothermal recovery for each of the five recovery stages. A constant, which depends on the stage, has been added to the value of  $\log(\text{time})$  to permit the display of the results for all the stages in one figure.

Here, the fraction of unrecovered damage  $\phi$  for a given stage is plotted versus  $\log(\text{time})$ . It is seen that the curves for stages I to IV are somewhat similar; stage V differs in that the recovery takes place over a longer period of time. It has not been possible to fit the isothermal recovery data for stages I-IV with any simple recovery model. In particular, first-order kinetics are not obeyed. A plot of  $1/\phi$  vs time for stage V is shown in Fig. 4. If a second-order chemical rate equation is obeyed, this should give a straight line. The data yield two straight lines which, in the simplest interpretation, implies a change in rate constant during the recovery process. The significance of this result is not clear at present.

The results of the analysis of the isochronal and isothermal recovery data for the activation energy for recovery are shown in Fig. 5, and the values of the activation energy are tabulated in Table I. The linearity of the  $\ln \Delta \tau_i$  vs  $1/T_i$  plots indicates that each of stages I to IV is characterized by a unique activation energy. Stage V is a possible exception since there is some deviation of the higher temperature points from the straight line. It is not known whether this is due to scatter in the data or some effect in the recovery, possibly connected with the behavior of the  $1/\phi$  vs time plot for stage V mentioned above.

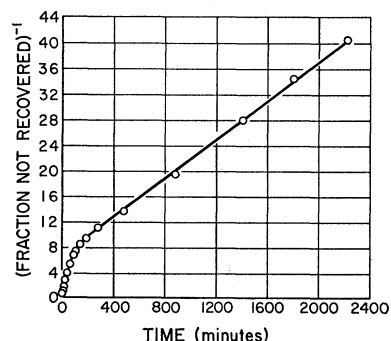


FIG. 4.  $1/\phi$  vs time for stage V.

TABLE I. Summary of recovery data.

Stage	Center temperature (°K)	Fractional recovery	$E$ (ev)
I	90	0.232	$0.34 \pm 0.01$
II	150	0.615	$0.60 \pm 0.02$
III	175	0.034	$0.70 \pm 0.02$
IV	210	0.027	$0.79 \pm 0.02$
V	275	0.092	$0.96 \pm 0.03$

In the present work, the same sample was used in obtaining the isothermal and isochronal data since it was possible to almost completely anneal out the damage from a given irradiation and then reproduce closely the necessary carrier-concentration change in a second irradiation. When isothermal or isochronal recovery in a given stage was measured more than once, good duplication of the results was obtained, indicating the above procedure of using the same sample for both the isothermal and isochronal measurements is valid.

### C. Stages I and II

#### 1. Evidence for Close Pairs

Despite the fact that stages I and II did not follow first-order kinetics, there are many indications from the data that these stages involve the annihilation of close interstitial-vacancy pairs. Since the same damage rate was observed at  $4^\circ$  and  $78^\circ\text{K}$  and no recovery was observed in the interval between these temperatures, it seems that the defects present at the beginning of stage I must be those initially produced by the irradiation unless migration of defects has taken place at helium temperature or it is possible for a change in the defect structure to occur without producing a change in the Hall coefficient and resistivity.

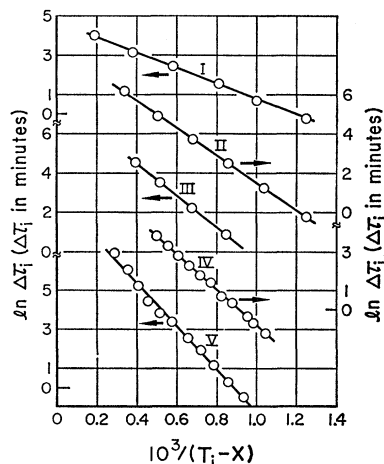


FIG. 5. A plot of  $\ln \Delta\tau_i$  vs  $1/T_i$  for each of the recovery stages. The scale for  $\ln \Delta\tau_i$  is indicated by the arrow for each of the stages.  $X$  takes the following values: stage I, 10; stage II, 6; stage III, 5; stage IV, 4; and stage V, 3.

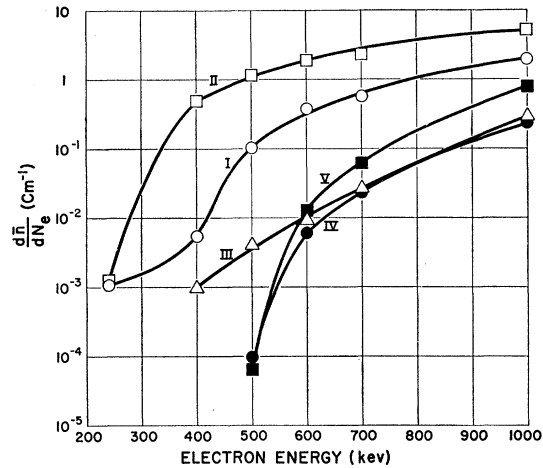


FIG. 6. (Carriers  $\text{cm}^{-3}$  removed from the conduction band)/(number of bombarding electrons  $\text{cm}^{-2}$ ),  $d\bar{n}/dN_e$ , for each recovery stage as a function of the incident energy of the bombarding electrons.

Figure 6 shows the results of an experiment in which the total damage recovering in each stage was measured as a function of bombarding electron energy.<sup>14</sup> These results show that separate threshold energies exist for the production of damage in the different stages. In particular, stages I and II have different thresholds or at least have their maximum rates of increase in different energy regions. It is possible that the "tail" on the curve for stage I may be due to a different damage production mechanism, and this is being investigated. The low values of threshold energy for these stages is consistent with the formation of close interstitial-vacancy pairs. The distribution of damage between the stages has been found to be independent of the integrated flux over the range from  $1.4 \times 10^{14}$  to  $1.2 \times 10^{15}$  electrons  $\text{cm}^{-2}$  at 1.0 Mev. This implies that the damage recovering in the higher temperature stages does not develop in a nonlinear manner from that recovering at lower temperatures and, therefore, that it is sensible to present data in the form shown in Fig. 6. It also indicates that multiple defects such as divacancies or di-interstitials are not products of any of the recovery stages since the number of such products would be a nonlinear function of the defect concentration. This would result in a change in the fraction of damage recovering in each of the stages related by such a process, with flux.

Figure 6 shows that almost 99% of the damage produced by 0.4-Mev irradiation recovers in stage II. The pre-irradiation values of both the Hall coefficient and resistivity are restored by this recovery, implying strongly that interstitials and vacancies recombine to

<sup>14</sup> The values of  $d\bar{n}/dN_e$  in Fig. 6 do not agree with those for low bombarding electron energies given in reference 5. The source of this discrepancy is not known; however, the present values are the correct ones. They agree with recent measurements in samples with  $n_0 = 10^{14} \text{ cm}^{-3}$  and with the shape of Fig. 1 in reference 5.

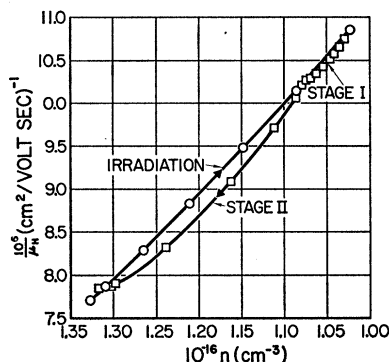


Fig. 7. Change in reciprocal Hall mobility during irradiation and annealing as a function of carrier concentration. Irradiation was at 0.7 Mev so that recovery was principally in stages I and II.

restore the pre-irradiation condition of the sample. It is not possible to obtain the same type of data for stage I; however, consideration of the mobility changes during irradiation and recovery indicates that this is also true of stage I recovery.

Figure 7 shows the change in the reciprocal of Hall mobility vs carrier concentration during irradiation at 0.7 Mev and subsequent annealing through stages I and II in which about 97% of the recovery took place. The recovery curve lies close to the irradiation curve with the Hall mobility and carrier concentration recovering together. The difference between the two curves will be discussed later. The significant point here is that the fraction of recovery of reciprocal Hall mobility in stage I was very nearly equal to the fraction of carrier-concentration recovery occurring in that stage, and the same was true of the recovery in stage II. This indicates that the recovery in stage I also consists of the recombination of interstitials and vacancies, since it is unlikely that any process which does not tend to restore the pre-irradiation condition of the sample would produce the observed relation between mobility recovery and carrier-concentration recovery. This restoration of the pre-irradiation condition of the sample during recovery in stages I and II together with the previously cited evidence that the primary defects are still present at the beginning of these stages rules out any formation of defect-impurity complexes, at least through the temperature region of these stages.

The question of the separation of the interstitials and vacancies which recombine in stages I and II is also of interest. If they lie within a capture radius of one another, the damage produced at different energies should show the same recovery kinetics. If two close-pair configurations recover in one stage as proposed later, this would still hold if the ratio of the concentrations of the two configurations did not depend strongly on energy. This may be the case when the bombardment energy is well above threshold. However, if interstitials and vacancies separated by a distance greater than the capture radius can recombine in one of these stages,

then a change in the energy of irradiation should produce a change in the observed recovery kinetics. This should be so, since increasing the energy of irradiation would increase the relative number of displacements beyond the capture radius, and these interstitial-vacancy pairs would be able to recombine in stages I or II and/or separate with recovery occurring at higher temperature. Figure 8 shows that isothermal recovery data for stage I or stage II after irradiation at 0.7 or 1.0 Mev can be superimposed for the respective stages by adjustment of the time scale. The indication from these data is, therefore, that the separation of the interstitials and vacancies which annihilate in stages I and II is less than a capture radius and that these interstitial-vacancy pairs must annihilate when the interstitial becomes mobile.

Further evidence for this point is the observation that damage is produced at 165°K at the same rate as if the sample were irradiated at 78°K and annealed to 165°K. This suggests that the defects stable above 165°K cannot be products of any of the defects which migrate and recombine in stages I and II, since these would be highly mobile at 165°K, so that one might expect the amount of any such products to be changed.

## 2. Failure of First-Order Kinetics

In view of the above arguments, the simplest interpretation of stages I and II would seem to be that they represent the annihilation of close interstitial-vacancy pairs, one of them representing the displacement of indium atoms, the other displacement of antimony atoms. First-order kinetics would be expected in this case, but it is not observed. If one tries to fit the isothermal recovery data to Eq. (2), the value of  $\gamma$  required is about 1.5.

## 3. Proposed Model for Stage II

Some progress toward an understanding of the recovery kinetics, in stage II at least, can be made from a consideration of recovery in samples with initial electron concentration  $n_0$  about  $10^{14} \text{ cm}^{-3}$ . In these

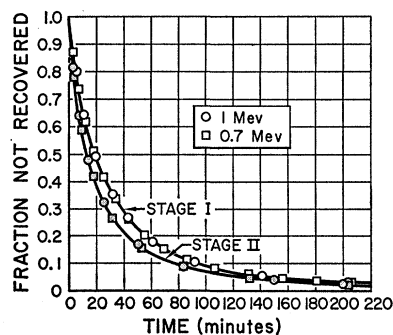


Fig. 8. Superposition of isothermal recovery in stages I and II for irradiations at 0.7 and 1.0 Mev. The time scale for the 1.0-Mev data was adjusted to superimpose them on the 0.7-Mev data.

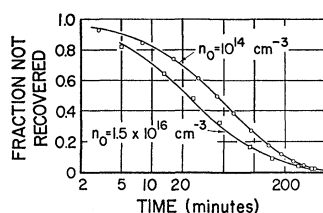


FIG. 9. Isothermal recovery in stage II. The solid curves are for the model described in the text for the respective values of  $n_0$ . The circles and squares are the experimental points.

samples it is found that the recovery in stages I and II takes place at a lower temperature and with slightly different recovery kinetics than in the samples with  $n_0 = 1.5 \times 10^{16} \text{ cm}^{-3}$ . The recovery in stage II is centered at  $130^\circ\text{K}$  with an activation energy of  $0.48 \pm 0.02 \text{ eV}$ .<sup>15</sup> The Fermi level in these samples is about  $0.025 \text{ eV}$  below the conduction band, suggesting that a possible explanation for the lower activation energy may be that one of the defect energy levels is only partially occupied and that there is an electrostatic attraction between the interstitial<sup>16</sup> thus ionized and its vacancy, resulting in a decrease in the potential-energy barrier for migration.<sup>17</sup>

The solution of the recovery problem for such a situation, in which the annihilation rate of ionized interstitials with vacancies is taken as proportional to the number ionized and the carrier concentration is always at its equilibrium value, is given in the Appendix. The result is of the form

$$\phi = e^{A(\phi-1)} e^{-Kt}, \quad (3)$$

where the constants are evaluated in the Appendix. The appearance of  $\phi$  in the exponential term results in a deviation from simple first-order kinetics; however, this deviation is not great enough to allow a fit to the data for stage II recovery with  $n_0 = 10^{14} \text{ cm}^{-3}$ .

In pursuing this approach further one is led to reconsider the assumption that the annihilation of the ionized interstitials with vacancies is a simple first-order process. The possibility that two jumps of the interstitial are rate determining or that two slightly different close-pair configurations may be decaying independently in the same recovery stage has been examined. The form of the recovery of reciprocal Hall mobility, shown in Fig. 7, gives an indication of the choice between these two possibilities. The mobility recovery proceeds more rapidly than the carrier-concentration recovery. This could be explained by two close-

pair configurations if they had slightly different scattering cross sections for electrons, the slower decaying pair having the smaller scattering cross section. On the other hand, if two jumps of the interstitial are rate determining and the potential-energy barrier for migration decreases as the defects approach each other, then, as the recovery nears completion, there are more interstitials in the first jump position than in the second. It seems likely that these pairs with the greater interstitial-vacancy separation should also have the greater scattering cross section for electrons, and the effect on the mobility recovery would be in the wrong direction to explain the data.

To test the suitability of the two-configuration model, the data for stage II recovery have been fitted to the equation

$$\phi = \beta\phi_1 + (1-\beta)\phi_2,$$

where  $\phi_1$  and  $\phi_2$  are of the form in Eq. (3). This represents the independent annihilation of two types of close-pair configuration with the recovery kinetics for both perturbed by the ionization considerations discussed above. The constant  $A$  is determined from the data, so that the fit is made by adjusting  $\beta$ ,  $K_1$ , and  $K_2$ . The result is shown in Fig. 9, and the fit is seen to be quite satisfactory. The constants required are  $\beta = 0.38$ ,  $K_1 = 0.0259 \text{ min}^{-1}$ , and  $K_2 = 0.00754 \text{ min}^{-1}$ . The difference in activation energy for the two pairs required to account for the difference in the  $K$ 's is about  $0.01 \text{ eV}$ , which is not sufficient to change the straight-line character of the  $\ln\Delta\tau_i$  vs  $1/T_i$  curve for this stage. If the ionization correction to the kinetics is ignored, the fit to the data is not as satisfactory. The proposed two close-pair configurations might be produced in one of two different ways. The first possibility is that stage II represents the displacement of only indium or only antimony atoms, and there are two close-pair configurations which recover in this stage. The other possibility is that the interstitial-vacancy configuration is similar, but one type is due to indium displacements and the other due to antimony displacements.

The appearance of  $n_f$ , the value of the carrier concentration after completion of stage II recovery, in the denominator of the expression for the rate constant  $K$  (see Appendix) indicates that there should be a change in the temperature  $T_c$  of the center (taken as the inflection point of the isochronal curve) of stage II if recovery is measured in samples of different  $n_0$  (for most irradiations,  $n_f$  was about equal to  $n_0$ ). The magnitude of the change can be calculated by requiring that  $n_0^{-1}e^{-E/kT_c}$  be the same for all values of  $n_0$ . This assures that  $K$  is equal at  $T_c$  for the different  $n_0$ . The calculated increase in  $T_c$  from  $n_0 = 10^{14} \text{ cm}^{-3}$  to  $n_0 = 10^{15} \text{ cm}^{-3}$  is  $7^\circ$ , which is in agreement with the observed difference for two such samples.

The situation is not as simple in extending the prediction of  $T_c$  to samples in which  $n_0 = 1.5 \times 10^{16} \text{ cm}^{-3}$ , since these samples are degenerate and the solution of the recovery problem in the Appendix is for the nondegenerate

<sup>15</sup> The value of  $E$  given here does not agree with that in reference 5. In the earlier work, the heater response was not as good as in the present experiments so that appreciable time and temperature corrections to the isothermal and isochronal recovery data were necessary. Therefore, it is felt that the present value is more reliable.

<sup>16</sup> The interstitial has been treated as the mobile defect earlier, and will continue to be so treated to facilitate the discussion. For the same reason, it will be treated as the defect which becomes ionized, being neutral before the ionization. Neither of these points is fundamental to the recovery model.

<sup>17</sup> Another situation in which removal of an electron from a defect results in a lowering of the barrier for recombination is discussed in reference 2. In this case, however, the recombination of the ionized defects proceeds more rapidly than the thermal ionization process so that the measured kinetics and activation energy are typical of the ionization process.

case. The inclusion of degeneracy in the problem results in the requirement that  $n_0^{-1}(N_c - 0.25n_0)e^{-E/kT_c}$  for degenerate samples be equal to  $n_0^{-1}N_c e^{-E/kT_c}$  for nondegenerate samples in order to have equal values of  $K$  at the different  $T_c$ . The predicted value of  $T_c$  for a sample with  $n_0 = 1.5 \times 10^{16} \text{ cm}^{-3}$  is  $147^\circ\text{K}$  which is slightly less than the observed value of  $150^\circ\text{K}$ . It is, therefore, difficult to understand why the recovery does not proceed with an activation energy of 0.48 eV rather than the observed value of 0.60 eV for  $n_0 = 1.5 \times 10^{16} \text{ cm}^{-3}$ . Presumably, this should correspond to the activation energy for recovery with no ionization of the interstitials. In this case, each of the two close-pair configurations should, by itself, obey first-order kinetics; and the observed recovery should be of the form

$$\phi = \beta e^{-K_1 t} + (1 - \beta) e^{-K_2 t}.$$

Figure 9 shows the data for a degenerate sample fitted to this equation. The values of the parameters required are  $\beta = 0.656$ ,  $K_1 = 0.0525 \text{ min}^{-1}$ , and  $K_2 = 0.00797 \text{ min}^{-1}$ . The fit is not as good as for the nondegenerate case discussed previously. Also, it would seem that the pair configuration that decayed more slowly in the nondegenerate case is now the faster decaying pair and vice versa. Thus, while the recovery model proposed above will explain some features of the recovery in stage II, it does not, at present, seem satisfactory in all details.

#### D. Stages III and IV

The data for stages III and IV are less complete. The isothermal recovery curves for these stages resemble those for stages I and II. The mobility data seem consistent with the annihilation of vacancies and interstitials, since the change in reciprocal Hall mobility vs  $\Delta n$  during recovery follows closely the change during an irradiation in which only the damage in stages III-V is measured, as shown in Fig. 10. The higher threshold energies and the above data suggest the possibility that stages III and IV represent the recombination of close pairs with a somewhat greater separation than those recombining in stages I and II. It is not possible to

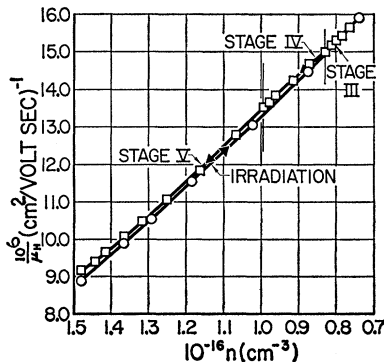


FIG. 10. Change in reciprocal Hall mobility during irradiation and annealing as a function of carrier concentration. The irradiation was performed at 1.0 MeV near  $80^\circ\text{K}$ . The sample was annealed to  $165^\circ\text{K}$  before measuring the data points on the irradiation curve so that only damage which recovers in stages III to V was measured.

determine whether or not these defects can also separate to produce the damage recovering in stage V from the present data, although the fact that the fraction of total recovery occurring in stage V is several times greater than that in stages III or IV may argue against this possibility.

#### E. Stage V

An exact interpretation of the recovery in stage V has not been made. It seems, however, from the time spread of the recovery that this must represent the movement of defects over greater distances than in the other stages. The second-order nature of the kinetics described earlier may indicate that the dominant process in the stage is the random recombination of interstitials and vacancies. If indium interstitials went only to indium vacancies and antimony interstitials to antimony vacancies, both the resistivity and Hall coefficient should return to their pre-irradiation values. Following stage V, the Hall coefficient usually returned to within about 0.1% of its pre-irradiation value, while there is a 1-2% change in resistivity remaining. The close return to the original values indicates that the annealing has largely restored the pre-irradiation conditions and that formation of an appreciable number of defect-impurity complexes is unlikely. The discrepancy between the amount of recovery of Hall coefficient and resistivity might be caused by the introduction of disorder in the sample due to some indium interstitials going to antimony vacancies and an equal number of antimony interstitials going to indium vacancies during stage V recovery. These defects might compensate each other, producing no carrier-concentration change. If they did this, they would be ionized and produce a mobility decrease and, therefore, an increase in the resistivity over the pre-irradiation value, as observed. The same effect could be caused by replacements produced directly by the irradiation.

#### V. SUMMARY

In summary, the following points concerning recovery of electron radiation damage in *n*-type InSb can be made from the present data.

1. The rate of production of defects is independent of the temperature of irradiation as long as it is a temperature at which the defects are stable.
2. Recovery occurs in five distinct stages between  $80^\circ$  and  $320^\circ\text{K}$ , with only a small change in resistivity remaining after completion of the fifth stage.
3. The recovery stages can be interpreted as due to the recovery of primary defects with essentially no formation of defect-impurity complexes.
4. Stages I and II seem to fulfill all the conditions expected for recovery of close interstitial-vacancy pairs with the exception that first-order kinetics is not explicitly obeyed.

#### ACKNOWLEDGMENTS

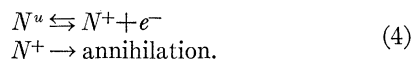
The author wishes to acknowledge the receipt of sample materials from H. P. R. Frederikse and R. K.



Willardson, the experimental assistance of P. W. Heindelman and A. M. Rosen, and helpful discussions with several of his colleagues at Atomics International.

### APPENDIX

To derive Eq. (3) in the text, let  $N$  be the total concentration of close pairs,  $N^+$  the concentration of close pairs with the interstitial ionized, and  $N^u$  the concentration with the interstitial unionized. We have the reactions



The rate of decay of the defects is given by

$$dN/dt = -K'N^+. \quad (5)$$

It is assumed, in Eqs. (4) and (5), that the decay of the pairs with ionized interstitials is the only mode of decay of the close pairs and that this decay is proportional to the number of pairs  $N^+$  with rate constant  $K'$ . From statistical considerations, if the electron redistribution is rapid compared to the decay of close pairs,

$$(N - N^+)/N^+ n = \lambda^{-1} N_c^{-1} e^{\epsilon/kT}, \quad (6)$$

where  $n$  is the carrier concentration,  $N_c = 2(2\pi kT m_n/h^2)^{3/2}$  is the standard expression for the density of states in

the conduction band,  $\epsilon$  is the ionization energy of the interstitial, and  $\lambda$  is a statistical weighting factor which depends on the degeneracies of the ionized and unionized states of the interstitial.<sup>18</sup> The carrier concentration is given by

$$n = n_f - \alpha N + N^+, \quad (7)$$

where  $n_f$  is the value of  $n$  on completion of recovery and  $\alpha$  is the number of electrons removed from the conduction band per close pair. From Aukerman's<sup>4,19</sup> work, it seems likely that  $\epsilon$  is not less than 0.04 eV, and it is reasonable to assume that  $N^+ \ll N$ . Making this assumption and substituting (5) and (6) in (7), we have

$$dN/dt = -K n_f N / (n_f - \alpha N),$$

where  $K = \lambda n_f^{-1} K' N_c e^{-\epsilon/kT}$ . This is easily integrated to give

$$\ln(N/N_0) = (\alpha N_0/n_f)(N/N_0 - 1) - Kt,$$

in which  $N_0$  is the value of  $N$  at  $t=0$ . This can be written in the form

$$\phi = e^{A(\phi-1)} e^{-Kt},$$

with  $A = \alpha N_0/n_f$ .

<sup>18</sup> W. Ehrenberg, *Electric Conduction in Semiconductors and Metals* (Oxford University Press, New York, 1958), p. 42.

<sup>19</sup> L. W. Aukerman, J. Appl. Phys. **30**, 1239 (1959).

## Effect of Hydrostatic Pressure on Ionic Conductivity in Doped Single Crystals of Sodium Chloride, Potassium Chloride, and Rubidium Chloride†\*

C. BALLARD PIERCE‡

Department of Physics, University of Illinois, Urbana, Illinois

(Received January 30, 1961; revised manuscript received May 8, 1961)

The effect of hydrostatic pressure up to 9000 kg/cm<sup>2</sup> on ionic conductivity in NaCl, KCl, and RbCl single crystals doped with divalent impurities has been studied over the temperature range 200° to 500°C. The conductivity in this temperature range is due almost entirely to the motion of extrinsic cation vacancies. The activation volume  $\Delta V_m$  for motion of the cation vacancies is  $7.7 \pm 0.5$  cc/mole in NaCl doped with CaCl<sub>2</sub> and  $7.0 \pm 0.5$  cc/mole in KCl doped with SrCl<sub>2</sub>. The results are in fair agreement with values predicted on the basis of Keyes's empirical expression relating activation volume to activation energy and isothermal compressibility. Sample materials were chosen with the view of testing for a correlation between activation energy and shear modulus. The small shear modulus in KCl and RbCl decreases with increasing pressure, while the reverse is true for NaCl. However, the data are not adequate to draw definite conclusions about such a correlation. The conductivity of RbCl doped with BaCl<sub>2</sub> increases by an order of magnitude at the phase transition from the NaCl to the CsCl structure. At 300°C, the transition occurs at 6100 kg/cm<sup>2</sup>.

### I. INTRODUCTION

IN spite of the large amount of effort that has been devoted to the study of point defects, vacancies and interstitials, in recent years, there are still several aspects of their properties and nature which are not

† This work was supported in part by the U. S. Atomic Energy Commission.

\* Based on a thesis submitted to the Graduate College of the University of Illinois in partial fulfillment of the requirements for the degree of Doctor of Philosophy, July, 1960.

‡ Now at Sandia Corporation, Albuquerque, New Mexico.

well understood. In particular, the extent of such a defect in a crystalline lattice, including relaxation and distortion of atoms or ions in the vicinity of a defect, is quite uncertain. Similarly, very little is known about the amount of lattice distortion necessary for diffusive motion of these defects in a solid. Experimentally, it is impossible at the present time to obtain a perfectly direct measure of this distortion. Theoretical calculations of necessity involve many approximations because of lack of detailed knowledge of interatomic forces.